Determination of Atomic Sites of Nb Dissolved in Metastable $Fe_{23}B_6$ Phase

Takahiro Nakamura[1, *], Hisato Koshiba[2], Muneyuki Imafuku[3], Akihisa Inoue[4]
and Eiichiro Matsubara[4]

[1]*Department of Materials Science, Tohoku University, Sendai 980-8577, Japan*
[2]*Alps Electric Co., Nagaoka 940-8572, Japan*
[3]*Nippon Steel Corporation, Futtsu 293-8511, Japan*
[4]*Institute for Materials Research, Tohoku University, Sendai 980-8577, Japan*

The primary metastable phase in the $Fe_{70}Nb_{10}B_{20}$ amorphous alloy is the complex fcc $Fe_{23}B_6$ phase with a large lattice parameter. The atomic site of Nb atoms in this metastable phase was determined by the anomalous X-ray scattering (AXS) method. Nb atoms in the metastable phase located at the similar position expected in the local structural unit in the amorphous state. Thus, the precipitation of the metastable phase does not require long-distance diffusion of Nb atoms in the amorphous matrix.

1. Introduction

Ferrous amorphous alloys, such as Fe–(Al, Ga)–(P, C, B, Si)[1] and Fe–Zr–B alloys,[2] with a large supercooled liquid region of more than 50 K were discovered. They exhibit good soft magnetic properties and are used as electro-magnetic materials. Based on these Fe-based systems, many of other Fe-based bulk amorphous alloys have been developed. The present Fe–Nb–B system is one of them. In this system, the nanometer-sized metastable $Fe_{23}B_6$ precipitates in the amorphous matrix before the equilibrium α–Fe, Fe_2B and Fe_3B phases are observed.[3–5] Since no such a metastable phase appears in the binary Fe–B system, it is expected that the formation of the metastable phase is closely related with Nb atoms in the ternary alloy. In this study, we determined the atomic sites of Nb atoms in the metastable phase by the anomalous X-ray scattering (AXS) method.

2. Experimental

Amorphous $Fe_{70}Nb_{10}B_{20}$ ribbons 0.03 mm thick and 3 mm wide were prepared by the single-roller melt spinning technique. Its thermal property was determined by the differential scanning calorimetry (DSC) at a heating rate of 0.67 K/s. The result of DSC is shown in Fig. 1. The glass transition followed by the appearance of the supercooled liquid region and the crystallization is clearly observed in the amorphous $Fe_{70}Nb_{10}B_{20}$ alloy. The glass transition temperature (T_g) and the crystallization temperature (T_X) are denoted in the figure. The clearly separated two exothermic peaks are observed in the DSC curves. They correspond to the precipitations of the metastable $Fe_{23}B_6$ phase and the equilibrium phases, respectively.[3]

The amorphous $Fe_{70}Nb_{10}B_{20}$ sample was annealed at 950 K for 1200 s under vacuum of 5×10^{-5} Pa for formation of the metastable phase $Fe_{23}B_6$. Several pieces of the ribbons of about 20 mm long were closely arranged on an aluminum
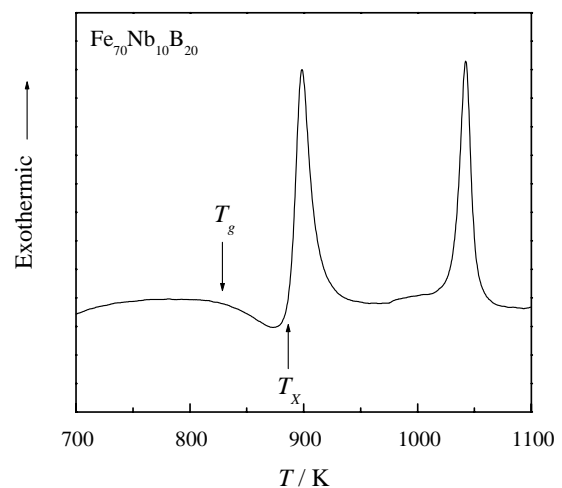

Fig. 1 The differential scanning calorimetry (DSC) profile of the amorphous $Fe_{70}Nb_{10}B_{20}$ alloy. The glass transition temperature (T_g) and the crystallization temperature (T_X) are indicated.

flame with a window of 15 mm by 10 mm for X-ray measurements. At low and high scattering angles, the symmetrical transmission and reflection geometries are adopted to reduce the influence of the sample flatness on scattering intensities.

AXS measurements were carried out at BL-9C in the Photon Factory of Institute of Materials Structure Science (IMSS), High Energy Accelerator Research Organization (KEK), Tsukuba, Japan. The energy differential intensity profile for Nb of the metastable phase was evaluated from the AXS intensities at 50 and 300 eV just below the Nb K absorption edge.

The X-ray atomic scattering factor is described by

$$f_j = f_j^0 + f_j' + i f_j'' \tag{1}$$

where f_j' and f_j'' are the real and imaginary parts of the anomalous dispersion term. The structure factor for *hkl* re-

flection, F_{hkl}, is given by

$$F_{hkl} = \sum_{j=1}^{N} f_j e^{2\pi i(hu_j + kv_j + lw_j)} \quad (2)$$

where u_j, v_j and w_j is the fractional coordinates of atoms. The intensity of a powder sample mounted on a diffractometer is

$$I = |F_{hkl}|^2 p \left(\frac{1 + \cos^2 2\theta}{2 \sin^2 \theta \cos \theta} \right) \frac{1}{2\mu}(1 - e^{-2\mu t/\sin \theta})e^{-2M} \quad (3)$$

where p is the multiplicity factor, 2θ the scattering angle, μ the liner absorption coefficient, t the thickness of the sample and e^{-2M} the temperature factor.

The AXS intensities of Fe$_{23}$B$_6$ were evaluated from a difference between two intensities calculated by eq. (3) at the two energies used in the present AXS measurements at the Nb K absorption edge. In the present study, several possible Nb sites that do not destroy the crystalline symmetry were assumed in the unit cell. The details will be gain in the next chapter. The Nb sites in the primary metastable phase were determined by comparing these calculated peak intensities with the observed AXS profile.

3. Results and Discussion

The AXS intensity profiles at 50 and 300 eV below the Nb K absorption edge and the differential profile are shown in Figs. 2(a) and (b). All peaks in Fig. 2(a) are identified by the Fe$_{23}$B$_6$ phase, that is the Cr$_{23}$C$_6$-type fcc. The structural data of the Fe$_{23}$B$_6$ crystal are summarized in Table 1. The Fe$_{23}$B$_6$ consists of 92 Fe and 24 B atoms with a lattice constant of 10.67 nm.[6]

Considering the composition of the Fe$_{70}$Nb$_{10}$B$_{20}$ alloy, the atomic sizes of Fe, Nb and B atoms, and the fact that Fe and Nb are metallic and B is non-metallic, we assumed that the Nb atoms replace the Fe atoms in the Fe$_{23}$B$_6$ crystal. From the atomic concentration of Nb, we can evaluate the number of Nb atoms replacing the Fe sites as 12. Without disturbing the crystalline symmetry by the replacement of Nb atoms, Nb atoms are placed at f- and/or h-sites, or randomly replaced all the Fe sites.

The result of the intensity calculation in the case that the Nb atoms randomly replace Fe atoms at the f-site, h-site and all sites are shown in Figs. 3(a), (b) and (d), respectively. They do not agree with the experimental result. On the other hand, in the case that the Nb atoms randomly replace the Fe atoms at the f- and h-sites, comparatively good agreement with the
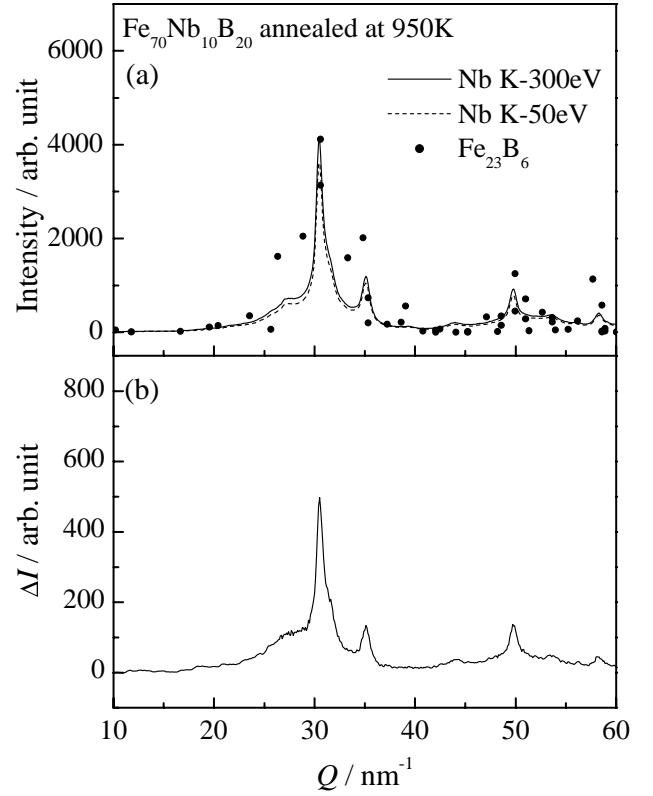

Fig. 2　(a) AXS intensity profiles at 50 eV (broken) and 300 eV (solid) below the Nb K absorption edges of the amorphous Fe$_{70}$Nb$_{10}$B$_{20}$ alloy annealed at 950 K for 1200 s. Full circle describes peak intensities of Fe$_{23}$B$_6$ calculated by eq. (3). (b) The energy differential profile defined as a difference between the two AXS intensities in (a).

Table 1　Numbers of symmetrical sites and coordinates of Fe and B atoms in Fe$_{23}$B$_6$.

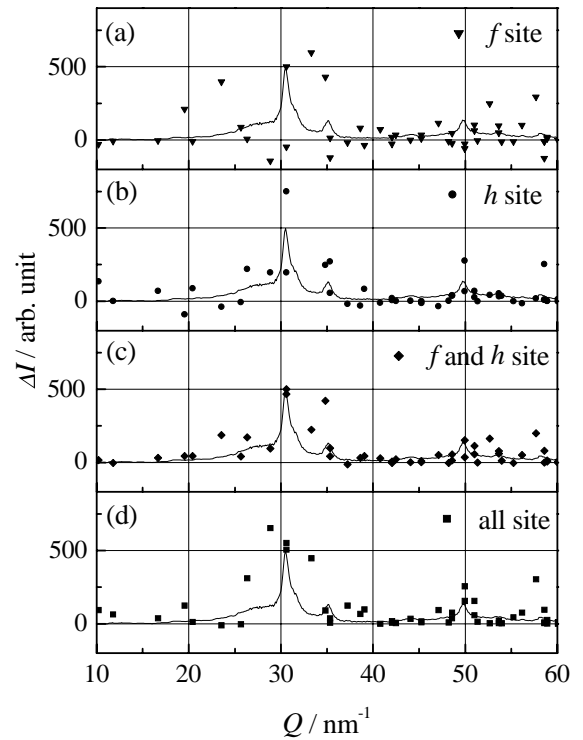| Element	Multi-plicity	Wyckoff letter	Coordinates		
			x	y	z
Fe	4	a	0	0	0
	8	c	1/4	1/4	1/4
	32	f	0.3820	0.3820	0.3820
	48	h	0	0.1699	0.1699
B	24	e	0.2751	0	0

Fig. 3　The energy differential intensity profile is compared with the peak intensities of Fe$_{23}$B$_6$ calculated by assuming the following cases. (a) Nb atoms randomly replace Fe atoms at the f-site (▼), (b) at the h-site (●), (c) at the f- and h-sites (◆), (d) at all Fe sites (■).
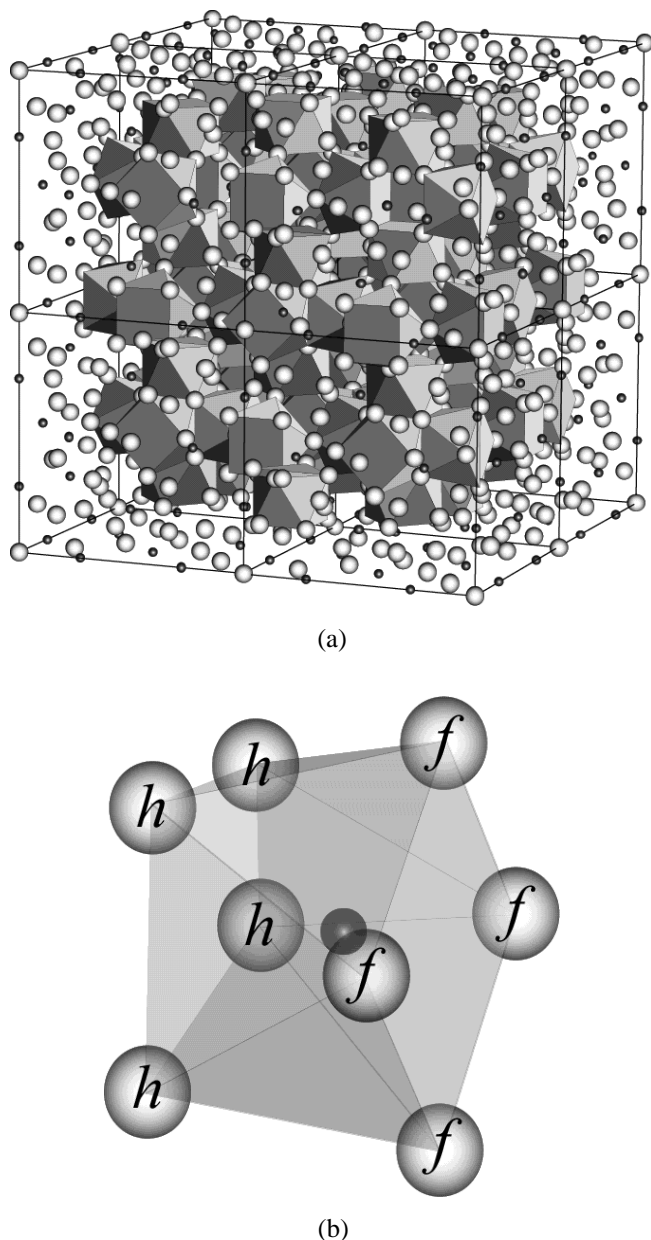
(a)

(b)

Fig. 4   (a) Schematic drawings of $2 \times 2 \times 2$ unit cells for $Fe_{23}B_6$. (b) The Archimedean prism structure in $Fe_{23}B_6$.

experimental result is seen, as shown in Fig. 3(c).

These analyses suggest that the Nb atoms mainly replace the Fe atoms at the f- and h-sites. The polyhedral clusters are included in the $Fe_{23}B_6$ unit cell (Fig. 4(a)). It is triangular prism that is composed of a B atom at the center and 8 Fe atoms at the vertices. The f- and h-sites correspond to the vertices of the triangular prism (Fig. 4(b)). It is noted that the local structural unit in the amorphous $Fe_{70}Nb_{10}B_{20}$ alloys is also the triangular prism and Nb atoms replace Fe atoms at the vertices of the prism.[7]

4.   Summary

The atomic sites of Nb atoms in the metastable phase were determined by the AXS method. Nb atoms mainly replaced the Fe atoms at the f- and h-sites. These sites correspond to the vertices of the triangular prism, and are the same position of the local structural unit in the amorphous state.

From these local structural resemblances between the metastable phase and the amorphous phase, it is plausible that for the formation of the metastable $Fe_{23}B_6$ phase, long-distance diffusion of Nb atoms is not required.

Acknowledgements

REFERENCES

1) A. Inoue and J. S. Gook: Mater. Trans., JIM **36** (1995) 1180–1183.
2) A. Inoue, T. Zhang, T. Itoi and A. Takeuchi: Mater. Trans., JIM **38** (1997) 359–362.
3) M. Imafuku, S. Sato, H. Koshiba, E. Matsubara and A. Inoue: Mater. Trans., JIM **41** (2000) 1526–1529.
4) M. Imafuku, S. Sato, H. Koshiba, E. Matsubara and A. Inoue: Scr. Mater. **44** (2001) 2369–2372.
5) M. Imafuku, C. Li, M. Matsushita and A. Inoue: Jpn. J. Appl. Phys. **41** (2002) 219–221.
6) J. L. C. Daams, P. Villars and J. H. N. van Vucht: *Atlas of Crystal Structure Types*, (1991).
7) T. Nakamura, E. Matsubara, M. Imafuku, H. Koshiba, A. Inoue and Y. Waseda: Mater. Trans., JIM **42** (2001) 1530–1534.